ELSEVIER

Synthetic Metals 116 (2001) 35–40

SYNTHETIC METALS

www.elsevier.com/locate/synmet

Interchain and intrachain exciton transport in conjugated polymers: ultrafast studies of energy migration in aligned MEH-PPV/mesoporous silica composites

Benjamin J. Schwartz*, Thuc-Quyen Nguyen, Junjun Wu, Sarah H. Tolbert

Department of Chemistry and Biochemistry, University of California, Los Angeles, CA 90095-1569, USA

Abstract

In this paper, we show how composite samples consisting of chains of the semiconducting polymer MEH-PPV embedded into the channels of oriented, hexagonal nanoporous silica glass allow control over energy transfer and exciton migration in the polymer. The composite samples are characterized by two polymer environments: randomly oriented and film-like segments with short conjugation-length outside the channels, and well aligned, long conjugation segments that are isolated by encapsulation within the porous glass. Ultrafast emission anisotropy measurements show that excitons migrate unidirectionally from the polymer segments outside the pores to the oriented chains within the pores, leading to a spontaneous increase in emission polarization with time. Because the chains in the pores are isolated, the observed increase in polarization can take place only by exciton migration along the polymer backbone. The anisotropy measurements show that energy migration along the backbone occurs more slowly than Förster energy transfer between polymer chains; transfer along the chain likely takes place by a thermally-activated hopping mechanism. Similar time scales for intra- and interchain energy transfer are also observed for MEH-PPV chains in solution. All the results provide new insights for optimizing the use of conjugated polymers in optoelectronic devices.

Keywords: Poly(phenylene vinylene) and derivatives; Time-resolved fast spectroscopy; Stimulated luminescence; Photoluminescence; Sol–gel processing; Micelles and solution self-assembly

Conjugated polymers are useful for devices because they combine the electrical and optical properties of traditional semiconductors with the mechanical and solution processing advantages of plastics [1–3]. One of the best studied conjugated polymers is poly[2-methoxy-5-(2′-ethyl-hexyloxy)-1,4-phenylene vinylene] (MEH-PPV), whose chemical structure and photoluminescence (PL) spectrum are shown in Fig. 1. A conjugated polymer chain is best thought of as a series of linked chromophores with a distribution of conjugation-lengths, because twists and bends of the chain lead to breaks in the conjugation. The confinement of the excited-state wavefunction (exciton) on shorter conjugation-length segments produces a blue-shifted absorption and luminescence, while the absorption and luminescence of longer conjugation-length segments is red-shifted. Following excitation, excitons rapidly move to the conjugated polymer segments that are the lowest in energy, leading to a structured and highly Stokes-shifted PL, as seen in Fig. 1a. Wavelength-dependent (site-selective) excitation experiments on conjugated polymers and oligomers are consistent with the basic picture of emission from low-energy segments following energy migration through an inhomogeneous density of states [4,5]. Time resolved PL experiments have observed the rapid decay of blue emission from high energy segments [6,7] and the delayed rise of red emission from low energy segments, [8] showing that energy transfer takes place in just a few picoseconds. Detailed modeling [9] of the observed energy migration is consistent with Förster transfer [10] (dipole–dipole coupling) as the predominant relaxation mechanism. Förster transfer on the time scale of a few picoseconds has also been observed in conjugated polymers doped with small amounts of a red-emitting guest [11–14]. All of this work makes it clear that energy transfer in conjugated polymers takes place rapidly and efficiently. None of these experiments, however, address the fundamental questions of how easily energy migrates along the backbone of a single polymer chain instead of between polymer chains, or how this energy flow can be controlled or directed.

In this paper, we show how control over energy flow can be achieved by aligning semiconducting polymer chromo-

* Corresponding author. Fax: +1-310-2064038.
E-mail address: schwartz@chem.ucla.edu (B.J. Schwartz).

0379-6779/01/$ – see front matter
PII: S0379-6779(00)00510-5

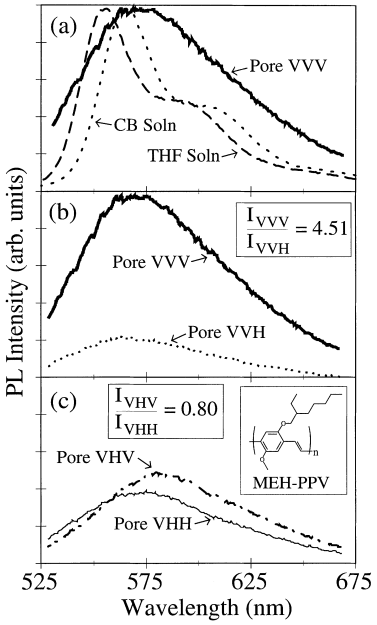

Fig. 1. (a) Steady-state photoluminescence (PL) spectra of MEH-PPV in different environments: chlorobenzene solution (CB, dashed curve), tetrahydrofuran solution (THF, dotted curve), and the mesoporous silica composite with excitation and collection polarizations parallel to the pore direction (VVV, heavy solid curve; see footnote 2). The three curves are scaled to the same maximum intensity for ease of comparison; (b) PL of MEH-PPV in the nanostructured composite with excitation light polarized along the pore direction. The heavy solid curve (VVV, same as (a)) shows emission collected polarized along the pore direction, while the dotted curve (VVH) is for emission collected polarized perpendicular to the pore direction; (c) PL of MEH-PPV in the nanostructured composite with excitation light polarized perpendicular to the pore direction. The dot-dashed curve (VHV) shows emission collected polarized along the pore direction, and the thin solid curve is for emission collected polarized perpendicular to the pores (VHH). The relative intensities of the four curves in (b) and (c) are as measured and have not been scaled. The inset shows the chemical structure of MEH-PPV.

phores on the nanometer scale via encapsulation into the hexagonally-arrayed channels of mesoporous silica glass [15,16]. The design of the system forces energy to flow along isolated polymer chains into the oriented portion of the composite material [17]. Thus, use of the composite allows us to separate the roles of interchain and intrachain energy transfer in conjugated polymers, providing valuable information for the optimization of polymer-based optoelectronic devices.

The main technique we use to examine the dynamics of energy transfer is time-resolved stimulated emission anisotropy. The details of our ultrafast apparatus, which has a ~200 fs time resolution, are described elsewhere [18–20]. Briefly, the samples are excited with a polarized ultrafast laser pulse centered at 490 nm, the peak of the MEH-PPV absorption spectrum. The polarized luminescence dynamics are measured via stimulated emission using a variably delayed probe pulse centered near the PL maximum of 590 nm. Energy transfer leads to loss of memory of the initial excitation polarization until eventually there is no difference in intensity for emitted light polarized either parallel ($\parallel$) or perpendicular ($\perp$) to that of the excitation laser. We monitor the remaining PL polarization memory via the time-dependent anisotropy, $r(t)$: [21]

$$r(t) = \frac{\parallel(t) - \perp(t)}{\parallel(t) + 2\perp(t)} \quad (1)$$

Because many of the optics in the experimental set-up have polarization-dependent reflectivities, the absolute magnitudes of the $\parallel$ and $\perp$ emission transients are somewhat difficult to measure. Thus, in the results presented below, we used the relative magnitudes of the polarized steady-state PL emission to properly scale the ratio of the integrated $\parallel$ and $\perp$ emission dynamics.

For MEH-PPV chains in solution, our recent work has shown that both the polymer conformation and the degree of interchain interaction can be controlled by changing the chemical nature of the solvent and the concentration of the polymer in solution, respectively [19,20]. The blue-shift of the emission from MEH-PPV in THF (Fig. 1a, dashed curve) relative to that in CB (Fig. 1a, dotted curve), for example, is the result of a tighter chain coil in THF that leads to a shorter average conjugation-length [19,20]. PL excitation and femtosecond pump-probe experiments show that MEH-PPV aggregation takes place more readily in CB than THF and that the degree of aggregation is higher at higher polymer concentration [19,20]. Thus, if primary mechanism for energy transfer and loss of emission polarization were exciton migration along the polymer backbone, as suggested in previous solution work on both other conjugated polymers [22,23] and MEH-PPV, [24] we would expect a much greater anisotropy decay in THF than CB due to the more highly coiled chain in THF. Instead, Fig. 2 shows that the opposite is observed: there is a greater loss of anisotropy for excited MEH-PPV in CB relative to THF. As we will argue in more detail below, we believe the rapidity of the anisotropy decay, along with the higher extent of aggregation of MEH-PPV in CB relative to THF [19,20], leads to the conclusion that the observed polarization loss is the result of *inter*chain energy transfer.[1]

If interchain Förster transfer dominates energy migration for conjugated polymers in solution, then what is the role of intrachain exciton transport in these materials? This question can be addressed by taking advantage of mesoporous silica/polymer host/guest chemistry [25–30] to produce composite materials with a strongly polarized polymer PL. In particular, we can make use of our previous work on incorporating MEH-PPV into the hexagonally-arrayed and aligned 22 Å diameter channels of a mesoporous silica

[1] Our definition of interchain transfer includes not only Förster transfer between conjugated segments on different chains, but also Förster transfer to conjugated segments that may be part of the same polymer chain: the operative definition is that the transfer is through space rather than intrachain along the polymer backbone. By interchain "contact", we refer simply to two conjugated segments (either on the same or different chains) that are physically located within a Förster transfer radius from each other.

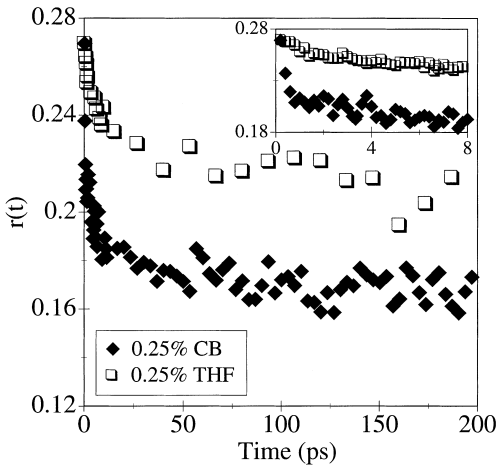

Fig. 2. Ultrafast stimulated emission anisotropy (Eq. (1)) of MEH-PPV in two different solution environments: chlorobenzene (CB, solid diamonds), and tetrahydrofuran (THF, open squares). For both solutions, the polymer concentration is 0.25% (w/v). The excitation and probe wavelengths are 490 and 590 nm, respectively. The inset shows the early time dynamics on an expanded scale.

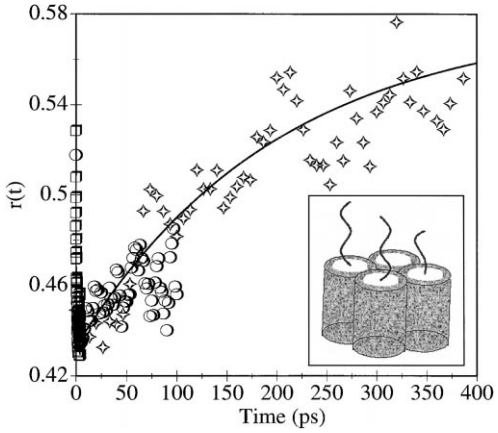

Fig. 3. Ultrafast stimulated emission anisotropy (Eq. (1)) of MEH-PPV encapsulated in mesoporous silica glass with the excitation pulse polarization parallel to the pore direction. Pump and probe wavelengths are the same as in Fig. 2. The solid curve in the figure is a 250 ps exponential rise. The different symbols represent scans taken with different time spacings between points. The inset shows a schematic of the pore system (pores vertically aligned) with one MEH-PPV polymer chain embedded per pore.

glass [30]. The synthesis makes use of a porous silica host that was aligned in a magnetic field via a silica/surfactant liquid–crystalline intermediate [31]. Following calcination and condensation of the silica host, [32] the resulting mesoporous glass is surface treated with organic groups to promote compatibility of the channel interiors with the polymer guest. MEH-PPV chains are incorporated from solution and the resulting composite is index-matched in a glycerol/propanol mixture to suppress scattering from the polycrystalline domain structure of the silica framework. Polarized steady-state PL (Fig. 1b and c)[2] shows that incorporation of MEH-PPV into the oriented porous silica host leads to a macroscopic alignment of the polymer chains, [30] as illustrated schematically in the inset to Fig. 3. The $\|:\perp$ emission ratio of 4.5:1 for the composite samples observed in Fig. 1b, which is quite a bit higher than the $\sim$1.3:1 ratio seen in MEH-PPV films, allows us to determine that over 80% of the polymer chromophores in the composite are aligned and inside the pores [30]. The remaining $\sim$20% of the chains are randomly oriented, either because the tails of the chains extend out to the tops of the pores, or because some of the polymer had adsorbed onto the outside of one of the silica domains. As discussed in detail elsewhere, ultrafast photo-induced absorption (PA) experiments can be used to show that the aligned polymer chains inside the pores are isolated in a solution-like environment, and that the randomly oriented chains outside the pores have a degree of interchain contact similar to that in the film [17].

Perhaps most important, though, is the fact that there is physically room for only one polymer chain per pore [30]. Thus, the polymer chains inside these composites are not just isolated but are individually encapsulated in a dielectric 2–3 nm thick, guaranteeing that energy transport cannot occur between chains[3].

The PL spectrum of the composite samples shown in Fig. 1 also tells us quite a bit about the polymer environment inside these materials. The increased breadth of the PL from chromophores inside the pores, VVV in Fig. 1a (see footnote 2) reflects an increase in the inhomogeneity of the polymer environment. In a solution or film sample, rapid (interchain) energy transfer causes excitons to migrate to the lowest energy sites, leading to a relatively homogenous emission characterized by vibronic structure. In the composite material, however, once excitons localize on an oriented segment within the pore, further energy transfer along the chain proceeds very slowly, as will be argued in more detail below. Förster transfer cannot take place inside the channels because the dipoles on adjacent segments are aligned head-to-tail instead of side-by-side. Thus, excitons inside the pores tend to localize on segments with a wide range of conjugation-lengths. In addition to this interior inhomogeneity, some of the composite sample PL comes from polymer segments outside the pores. In combination, the highly

[2] The notation used in Fig. 1 is that the first of the three letters indicates the orientation of the pores in the lab frame (always vertical (V) in this paper); the second letter (V or H) is the polarization of the excitation laser and the third V or H represents the polarization of the emitted light being probed.

[3] While Förster energy transfer between different chains in the channels is possible, we expect that Förster transfer inside the composite is inhibited due to the presence of the silica, which has a dielectric constant of $\sim$1.5. It is worth noting that conjugated polymer chains in adjacent pores are held to be parallel by the rigidity of the silica matrix. Thus, even if some energy transfer does take place between chains in neighboring pores, it would not cause a reorientation of the emission transition dipole and hence would not affect the results or conclusions drawn from the ultrafast anisotropy measurements.

inhomogenous distribution of chromophore sites both inside and outside the composite causes the vibronic structure of the PL to be washed out. In addition to being broader, the peak position of the PL from the polymer in the composite sample is red-shifted relative to that in solution (Fig. 1a), showing that the average conjugation-length of the chromophores inside the channels is longer than that in solution. This makes sense in light of the fact that incorporation into the channels forces the polymer chains to become straighter, increasing the conjugation-length.

To probe the fate of the emissive excitons created on the polymer chains, we use both steady-state and time-resolved polarized PL to monitor energy transfer in the composites. When exciting with light polarized perpendicular to the pore direction, more light is emitted polarized in the direction along the pores (Fig. 1c, dot-dashed curve VHV) than along the direction of excitation (Fig. 1c, thin solid curve VHH). This suggests that excitons on conjugated polymer segments outside the pores, which are preferentially excited by the light polarized against the pore direction, migrate to lower energy segments inside the pores where they emit light polarized along the pore direction. The presence of directional migration is also supported by the fact that the PL polarized parallel to the pores is red-shifted relative to that along the excitation direction.

Fig. 3 shows the emission anisotropy dynamics from the composite sample when the excitation laser is polarized along the pore direction. The initial value of the anisotropy, $r(0) = 0.53$, is double that in solution (cf Fig. 2), indicating a much greater polarization memory in the composite than in isotropic samples. On the basis of previous energy transfer studies, [6–14] we assign the initial loss of anisotropy in the first few picoseconds to interchain energy transfer between the ~20% of the chromophores in the film-like environment outside the pores. After the rapid decay is complete, we see an *increase* in the anisotropy which eventually reaches a value *greater* than $r(0)$ — the PL polarization spontaneously increases with time. The solid line in Fig. 3 is a fit to a 250 ps exponential rise.[4] As with the steady-state data in Fig. 1b and c, the only way to explain this increase in energy polarization is by migration of excitons from the coiled and non-aligned high-energy segments outside the pores to the straight and oriented low-energy segments encapsulated in the pores. Since the composite samples are designed to have room for only one chain per pore, exciton migration to chromophores inside the pores must take place along the polymer backbone. Thus, by forcing energy to flow along single polymer chains, the design of the composite takes energy deposited with random orientation outside the pores and directs it to the aligned chromophores within the pores, ultimately resulting in a PL polarization greater than that created by the original optical excitation. Thus, light energy with all polarizations is harvested by the ''antenna'' chromophores outside the pores and then funneled into the aligned polymer segments within the pores, in direct analogy to the photosynthetic reaction center. It is worth noting that simpler systems consisting of conjugated polymers aligned by tensile drawing [33–35] do not have the requisite nanoscale architecture to perform this type of directed energy transfer.

The key inference to be drawn from Fig. 3 is that exciton transport along the polymer backbone takes place on a time scale that is a few orders of magnitude slower than interchain transport via Förster transfer. This assignment of the fast anisotropy loss to interchain transfer and the slow anisotropy rise to exciton migration along the backbone is also supported by the PL anisotropy dynamics of MEH-PPV in solution. Fig. 4 compares the PL anisotropy decay of MEH-PPV in THF solution at both low (squares, same as in Fig. 2) and high (circles) concentrations. The chain conformation in these two solutions is the same, but the amount of interchain contact is increased at higher concentration [19,20]. The increasing amplitude of the fast anisotropy loss with increasing concentration (Fig. 4) supports the assignment of polarization scrambling due to interchain energy transfer between those conjugated polymer segments that are physically located within a Förster transfer radius (whether or not the chromophores are physically part of the same chain (see footnote 1)). At low concentration, once the energy has migrated sufficiently, interchain energy transfer ceases because there are no lower energy segments close enough for Förster transfer to take place. Excitons can continue to move along the polymer backbone, but Fig. 3 makes it evident that they do so quite slowly, on a time scale of a few hundred picoseconds: there is insufficient time for the exciton to move enough distance during its lifetime to

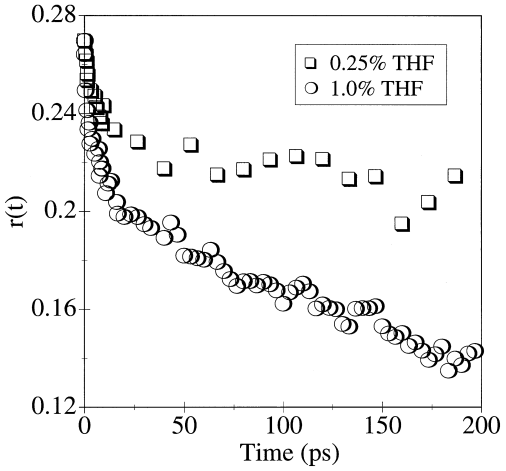

Fig. 4. Ultrafast stimulated emission anisotropy (Eq. (1)) of MEH-PPV at two different concentrations in THF solution: 0.25% (w/v) (open squares, same as those in Fig. 2), and 1.0% (w/v) (open circles) The excitation and probe wavelengths are the same as in Figs. 2 and 3.

[4] We choose a single exponential fit solely to define the characteristic time for the anisotropy increase. We do not feel that the signal-to-noise ratio of the anisotropy at long times (which, when most of the excitons have decayed is computed from the ratio of two small numbers) justifies fitting to a more complex model with additional parameters.

significantly change the orientation of the transition dipole. This produces the long-time anisotropy plateaus for the low concentration solutions shown in Fig. 2. At high concentration, on the other hand, after the rapid interchain transfer is complete, the likelihood of finding a lower-energy chromophore on a nearby chain within the Förster radius increases as excitons migrate for small distances along the backbone. This allows additional interchain transfer to occur, rate-limited by the intrachain energy migration on the ~250 ps time scale.

Why is intrachain energy transport so slow? We believe the reason is that migration along the backbone requires communication between polymer segments that are separated by a region of broken conjugation. This means that the chain segments must physically reorient (''iron out the kinks'') to allow exciton transport from one conjugated region to the next. As mentioned earlier, Förster transfer is ineffective for intrachain transport because the dipoles on adjacent segments lie head-to-tail. Thus, intrachain energy migration is slow because the necessary physical reorientation of the polymer backbone takes time, a process that is likely to be thermally activated. We are presently performing temperature-dependent emission anisotropy experiments not only to verify that the best description of intrachain exciton migration is that of a thermally-activated hopping process, but also to determine the activation energy for intrachain transport. In the interim, we can crudely estimate the intrachain exciton diffusion coefficient by noting that the exciton has to migrate far enough in ~250 ps to significantly reorient the direction of its transition dipole. The distance between adjacent polymer chain segments that lie in different directions can be approximated by the polymer's persistence length, which for MEH-PPV in solution has been measured by light scattering to be ~6 nm [36]. If we assume that the exciton migrates this distance in ~250 ps, we can estimate the exciton diffusion constant along the backbone to be $\sim 2 \times 10^{-5}\,\mathrm{cm}^2/\mathrm{s}$.

The fact that exciton transport along the conjugated polymer backbone is much slower than energy transfer between chains has profound consequences for devices based on these materials. Recent work by Warman and co-workers has found that the intrachain mobility of electrons and holes on MEH-PPV is orders of magnitude larger than the mobility observed by time-of-flight measurements in conjugated polymer devices [37]. This suggests that polaron transport is slow between chains but rapid along the conjugated polymer backbone, the opposite of what we have found here for exciton transport. Together, these results suggest that the efficiency of devices based on conjugated polymers can be greatly increased with proper control over interchain interactions [19,20]. In most polymer-based devices, the current that can be transported through the active polymer film is limited by the slow hopping of carriers between chains. Once the carriers do recombine, the resulting electroluminescence can be easily quenched by rapid interchain exciton migration to a low energy defect or trap site. On the other hand, if electrical contact could be made to single polymer chains such as those encapsulated in the mesoporous glass, the resulting device would have efficient charge transport since the current would not be limited by hopping of carriers between chains. The injected carriers in such a device would be forced to recombine on a single chain, reducing the probability of quenching at defect sites since the newly formed exciton would not be able to migrate a significant distance along the backbone during its lifetime. It also may be possible to significantly enhance device efficiency by utilizing energy transfer into the defect-free polymer segments within the pores even without direct electrical contact to single chains. Clearly, with sufficient control over the interaction between chains, there is an enormous potential waiting to be tapped for use of conjugated polymers in a variety of optoelectronic applications.

Acknowledgements

Acknowledgement is made to the donors of the Petroleum Research Fund, administered by the ACS (Grant nos. 32773-G6 and 33715-G5), to the National Science Foundation (DMR-9971842) and to the office of Naval Research (grant no. N00014-99-1-0568) for support of this work. B.J.S. is a Cottrell Scholar of Research Corporation and an Alfred P. Sloan Foundation Research Fellow.

References

[1] R.H. Friend et al., Nature 397 (1999) 121.
[2] G. Gustafsson et al., Nature 357 (1992) 477.
[3] L.J. Rothberg, A.J. Lovinger, J. Mater. Res. 11 (1996) 3174.
[4] R. Kersting et al., Phys. Rev. Lett. 70 (1993) 3820.
[5] U. Lemmer et al., Chem. Phys. Lett. 209 (1993) 243.
[6] G.R. Hayes, I.D.W. Samuel, R.T. Phillips, Phys. Rev. B 52 (1995) R11569.
[7] R. Kersting et al., J. Lumin. 72–74 (1997) 936.
[8] C. Warmuth et al., J. Lumin. 76–77 (1998) 498.
[9] R. Kersting et al., J. Chem. Phys. 106 (1997) 2850 (and references therein).
[10] T. Förster, Ann. Physik. 2 (1948) 55.
[11] P. Bolivar et al., Chem. Phys. Lett. 245 (1995) 534.
[12] A. Dogariu, R. Gupta, A.J. Heeger, H. Wang, Synth. Met. 100 (1999) 95.
[13] G. Cerullo et al., Synth. Met. 101 (1999) 306.
[14] M. Wohlgenannt et al., Chem. Phys. 227 (1998) 99.
[15] C.T. Kresge et al., Nature 359 (1992) 710.
[16] J.S. Beck et al., J. Am. Chem. Soc. 114 (1992) 10834.
[17] T.-Q. Nguyen, J. Wu, V. Doan, B.J. Schwartz, S.H. Tolbert, Science 288 (2000) 652.
[18] V. Doan, V. Tran, B.J. Schwartz, Chem. Phys. Lett. 288 (1998) 576.
[19] T.-Q. Nguyen, V. Doan, B.J. Schwartz, J. Chem. Phys. 110 (1999) 4068.
[20] T-Q. Nguyen, I.B. Martini, J. Liu, B.J. Schwartz, J. Phys. Chem. B 104 (2000) 237.
[21] C.R. Cantor, P.R. Schimel, in: W.H. Freeman (Ed.), Biophysical Chemistry Part II, 1980, p. 474.
[22] A. Watanabe, T. Kodaira, O. Ito, Chem. Phys. Lett. 273 (1997) 227.
[23] A. Ruseckas et al., J. Lumin. 76–77 (1998) 474.
[24] J.Z. Zhang et al., J. Chem. Phys. 106 (1997) 3710.

[25] C.-G. Wu, T. Bein, Science 266 (1994) 1013.
[26] C.-G. Wu, T. Bein, Science 264 (1994) 1757.
[27] K. Moller, T. Bein, R.X. Fischer, Chem. Mater. 10 (1998) 1841.
[28] K. Moller, T. Bein, R.X. Fischer, Chem. Mater. 11 (1999) 665.
[29] H.L. Frisch, J.E. Mark, Chem. Mater. 8 (1996) 1735.
[30] J.J. Wu, A.F. Gross, S.H. Tolbert, J. Phys. Chem. B 103 (1999) 2374.
[31] A. Firouzi et al., J. Am. Chem. Soc. 119 (1997) 9466.
[32] S.H. Tolbert, A. Firouzi, G.D. Stucky, B.F. Chmelka, Science 278 (1997) 264.
[33] C. Weder, C. Sarwa, C. Bastiaansen, P. Smith, Adv. Mat. 9 (1997) 1035.
[34] G.R. Hayes, I.D.W. Samuel, R.T. Phillips, Phys. Rev. B 56 (1997) 3838.
[35] M. Yan et al., Phys. Rev. B 49 (1994) 9419.
[36] C.L. Gettinger, A.J. Heeger, J.M. Drake, D.J. Pine, J. Chem. Phys. 101 (1994) 1673.
[37] R.J.O.M. Hoofman, M.P. deHaas, L.D.A. Siebbeles, J.M. Warman, Nature 392 (1998) 54.